RAPID COMMUNICATIONS

PHYSICAL REVIEW E VOLUME 52, NUMBER 3 SEPTEMBER 1995

Chaoticity spectrum in Hamiltonian systems with many degrees of freedom

Maira D'Alessandro
Forum–Istituto Nazionale per la Fisica della Materia, Physics Department, University of Florence, Largo E. Fermi 2, 50125 Florence, Italy

Alexander Tenenbaum*
Physics Department, "La Sapienza" University, Piazzale A. Moro 2, 00185 Rome, Italy
(Received 13 February 1995)

We present a diagnostic tool to analyze the chaoticity of single degrees of freedom: the *coherence angles*, which measure the angular distance between any physically relevant direction and the direction of maximum expansion in the tangent space. They allow at the same time a detailed characterization and a synoptic view of the dynamical behavior of a system with many degrees of freedom. Results are presented for two- and three-dimensional Lennard-Jones lattices, which show a nontrivial structure of the spectrum of coherence angles.

PACS number(s): 05.45.+b, 63.20.−e, 63.70.+h

The extended and variegated evidence for chaotic or ordered dynamical behavior in Hamiltonian systems has been recently put under a comprehensive point of view through the concept of strong stochasticity threshold (SST) [1,2]. The SST separates in the phase space regions characterized by a highly chaotic dynamics (Anosov-type diffusion) from regions of highly ordered dynamics, where only a weak chaos can be detected (Arnold-type diffusion). In the phase space region where the transition from one regime to the other takes place, detailed analysis of the dynamics shows that different degrees of freedom (DOFs) in one and the same state of the system may be characterized by very different behaviors, ranging from chaotic to ordered [3,4]. This coexistence extends into the region of weak chaos, where a global chaoticity—due to the presence of few chaotic DOFs—may hide the existence of many other ordered DOFs. Is a similar situation likely to be present also in the region of strong chaos? Up to now little attention has been given to this problem, and anyway in systems with few DOFs. The reason is that the usual indicators of order and chaos are either of global nature (Lyapunov exponents, fractal dimension, spectral entropy), or become soon impracticable when the number of DOFs becomes large (Poincaré maps, auto- and cross-correlation functions).

In this paper we introduce a diagnostic tool which, while being easily computable, allows a detailed dynamical characterization of each DOF and, at the same time, a synoptic description of the system as a whole. By means of this tool the DOFs endowed with the highest chaoticity may be easily singled out. We will show—taking as an example two- and three-dimensional (2D and 3D) Lennard-Jones microcrystals in a temperature range around the SST—that in a Hamiltonian system with many DOFs, chaos can be driven by few of them even above the SST.

It is well known that a measure of the degree of chaoticity of a dynamical system is the rate of divergence in the phase space of initially nearby trajectories, computed through the Lyapunov exponents. We call *coherence* the characteristic of trajectories with zero or low divergence, and we are interested in the coherence of single, physically relevant DOFs. This property can be quantified—in the tangent space of the dynamical system—through the average angle between the direction corresponding in that space to each DOF, and the direction corresponding to the maximum Lyapunov exponent. These *coherence angles* turn out to be easily computable and stable. Let Φ^t: $\mathbb{R}^m \to \mathbb{R}^m$ be a flow generated by the set of differential equations $\dot{\mathbf{x}} = \mathbf{f}(\mathbf{x})$, $\mathbf{x} \in \mathbb{R}^m$ (where $\mathbb{R}^m$ represents the phase space); the linear evolution of a generic vector $\mathbf{w} \in T\mathbb{R}^m_{\mathbf{x}}$, the tangent space in $\mathbf{x}$, is given by

$$\dot{w}_i(t) = \sum_{j=1}^{m} \frac{\partial f_i}{\partial x_j} w_j(t). \tag{1}$$

Oseledec [5,6] proved that for almost all initial conditions $\mathbf{x}(0)$ there is a base $\{\hat{\mathbf{e}}_i\}$ in $T\mathbb{R}^m_{\mathbf{x}(0)}$ such that

$$\mathbf{w}(t) = \sum_{i=1}^{m} |\mathbf{w}(0)| \mathbf{c}_i(t) \hat{\mathbf{e}}_i \exp(\tilde{\lambda}_i t) \tag{2}$$

for large enough times. $\tilde{\lambda}_1 \geq \tilde{\lambda}_2 \geq \cdots \geq \tilde{\lambda}_m$ are the Lyapunov exponents; the matrices $\mathbf{c}_i(t)$ entail a possible time dependence weaker than the exponential one, and the rotation of the base $\{\hat{\mathbf{e}}_i\}$ generated by the evolution equations (1). If $\lambda_1 > \lambda_2 > \cdots > \lambda_s$ ($s \leq m$) are the s different values of the set $\{\tilde{\lambda}_i\}$, then from (2) it follows

$$\mathbf{w}(t) = \sum_{i=1}^{s} \mathbf{a}_i(t) \exp(\lambda_i t) \equiv \mathbf{b}(t) \exp(\lambda_1 t),$$

where $\mathbf{a}_i(t) = \Sigma_j |\mathbf{w}(0)| \mathbf{c}_j(t) \hat{\mathbf{e}}_j$ for all j: $\tilde{\lambda}_j = \lambda_i$, and $\lim_{t\to\infty} \mathbf{b}(t) = \mathbf{a}_1(t)$ for almost all $\mathbf{w}(0)$. We imagine decomposing the phase space $\mathbb{R}^m$ into n subspaces, $S_1, S_2, \ldots, S_n$ ($n \leq m$), corresponding to a set of DOFs which are physically interesting for the study of the system. For the sake of simplicity we suppose that they are orthogo-

*Author to whom correspondence should be sent. Electronic address:: tenenbaum@roma1.infn.it

nal [7]. This phase space decomposition will induce an analogous decomposition of the tangent space $T\mathbb{R}^m$ in n subspaces $TS_1, TS_2, \ldots, TS_n$. Now we define the *coherence angles* (CAs) $\alpha^{(l)}$ through

$$\cos^2\alpha^{(l)} = \lim_{t\to\infty} \frac{1}{t}\int_0^t \frac{|\mathbf{w}^{(l)}(t')|^2}{|\mathbf{w}(t')|^2}\, dt'$$

where $\mathbf{w}^{(l)}(t)$ is the projection of $\mathbf{w}(t)$ on TS_l. It is evident that $\mathbf{w}^{(l)}(t)\to\mathbf{a}_1^{(l)}(t)\exp(\lambda_1 t)$ for large times, where $\mathbf{a}_1^{(l)}(t)$ is the projection of $\mathbf{a}_1(t)$ on TS_l. Only if $\mathbf{a}_1(t)$ were orthogonal to TS_l, one would have $\mathbf{w}^{(l)}(t)\to\mathbf{a}_2^{(l)}(t)\exp(\lambda_2 t)$ for large times. So we have that

$$\cos^2\alpha^{(l)} = \lim_{t\to\infty} \frac{1}{t}\int_0^t \frac{|\mathbf{a}_1^{(l)}(t')|^2}{|\mathbf{a}_1(t')|^2}\, dt'$$

and each $\alpha^{(l)}$ represents an effective angle between the subspace TS_l and the maximum expansion subspace. The TS_l are fixed; the maximum expansion subspace—to which $\mathbf{a}_1(t)$ belongs—depends only on the phase space representative point, and oscillates around its average orientation in $T\mathbb{R}^m_{\mathbf{x}(t)}$ [8]. It follows that the computation of the CAs should have a weak dependence on the initial conditions in tangent space, that is on the choice of $\mathbf{w}(0)$. As $\Sigma_{l=1}^n \cos^2\alpha^{(l)}=1$ we define an *average* coherence angle α through $\cos\alpha=1/\sqrt{n}$. Deviations of $\cos\alpha^{(l)}$ from $\cos\alpha$ will give a measure of the chaoticity degree of each subspace TS_l when compared with the average value. Indeed, any DOF corresponding to a $\cos\alpha^{(l)}>0$ will *asymptotically* diverge with a rate given by λ_1. Nevertheless, it is important to characterize the level of chaoticity of the DOFs in the *medium time regime*. By this we mean a scale typical for the time needed by a generic tangent vector to reorient in the direction of maximum expansion, that is $\mathbf{a}_1$. This regime is physically relevant, since experiments (real, or on a computer) performed on this time scale often detect phenomena due to differences of chaoticity among the DOFs. In the medium time of a dynamical evolution, each DOF will be characterized by an effective expansion rate, which will be a mixture of rates relative to all Lyapunov exponents. For the DOFs characterized in the tangent space by a small angle $\alpha^{(l)}$ with the first Lyapunov vector, this effective rate will be near to the maximum one; in general, values of $\cos\alpha^{(l)}$ higher than $\cos\alpha$ mean a higher chaoticity than the average.

We have used the CAs to analyze the dynamics of simple microcrystals, as an example of Hamiltonian systems with many DOFs. The dynamical characterization of any condensed matter system has, as a preliminary step, the identification of a set of *appropriate* coordinates, i.e., coordinates which are suitable to show up the peculiar phenomenology due to the existence (and possible coexistence) of ordered and chaotic dynamical regimes. For lattices a set of appropriate coordinates is already known to be that of the normal modes, while the behavior of Cartesian atomic coordinates does not exhibit a significant difference above and below the SST. In the following, the DOFs taken into account will therefore be the normal modes of a lattice. The subspaces $S_1, \ldots, S_n$ corresponding to the normal modes are orthogonal, as required.

In order to allow comparison with previous work [3,4] we have first chosen for the simulation a 2D system composed of N^2 particles of mass M ($N=8$), arranged on a square lattice with square cells of side d, surrounded by a border of fixed particles. Each particle is bonded to the four first neighbors by a Lennard-Jones (LJ) potential:

$$V(r)=4\varepsilon\left[\left(\frac{\sigma}{r}\right)^{12}-\left(\frac{\sigma}{r}\right)^{6}\right] ;$$

$V(r)$ has its minimum at $r_0=2^{1/6}\sigma$. Let us denote by $x^0_{l\,m}$ and $y^0_{l\,m}$ ($l,m=1,8$) the coordinates of site (l,m) and by $u^x_{l\,m}$ *e* $u^y_{l\,m}$ the displacements of the particles from their equilibrium positions. The normal-mode coordinates are defined by

$$q^x_{hk}=\frac{2}{N+1}\sum_{l,m=1}^{N} u^x_{lm}\sin\left(\frac{h\pi\, l}{N+1}\right)\sin\left(\frac{k\pi m}{N+1}\right) ,$$

$$q^y_{hk}=\frac{2}{N+1}\sum_{l,m=1}^{N} u^y_{lm}\sin\left(\frac{h\pi\, l}{N+1}\right)\sin\left(\frac{k\pi m}{N+1}\right) ,$$

where $h,k=1,N$. In these coordinates the Hamiltonian of the system is

$$H=\frac{M}{2}\sum_{h,k=1}^{N}[(\dot q^x_{hk})^2+(\omega^x_{hk})^2(q^x_{hk})^2+(\dot q^y_{hk})^2 + (\omega^y_{hk})^2(q^y_{hk})^2]+H' ,$$

where H' is the Hamiltonian of the coupling, which is negligible at sufficiently low energies, and $\omega^x_{h\,k}$, $\omega^y_{h\,k}$ are the angular frequencies of the normal modes:

$$(\omega^x_{hk})^2=(\omega^y_{kh})^2=\frac{4}{M}\left[K_L\sin^2\frac{\pi\, h}{2(N+1)}+K_T\sin^2\frac{\pi\, k}{2(N+1)}\right],$$

$$K_T\equiv\frac{1}{r}\frac{\partial V}{\partial r}\bigg|_d , \qquad K_L\equiv\frac{\partial^2 V}{\partial r^2}\bigg|_d .$$

We have considered two different cases:

(i) $d_1=r_0$, which corresponds to zero pressure at zero temperature. In this case $K_T=0$. There are only N distinct frequencies ($\omega^x_{hk}=\omega^y_{kh}\equiv\omega_h$) ranging from 0.3789 to 2.1491 in LJ reduced units. The normal modes are naturally divided into N groups, each including $2N$ modes of equal frequency. The total energy of the system may now be written as the sum of the energies E_h of each group of modes, plus the energy of the coupling due to the H' term; one has

$$E_h=\frac{M}{2}\sum_{k=1}^{N}[(\dot q^x_{hk})^2+(\omega^x_h q^x_{hk})^2+(\dot q^y_{kh})^2+(\omega^y_h q^y_{kh})^2] .$$

In this case, the eight group energies E_h will be the relevant DOFs. In fact, as described in [4], modes of equal frequency rapidly exchange their energy, always providing a good energy partition inside the group; therefore, the energies of the groups become the relevant DOFs.

(ii) Compressing the system ($d<r_0$), one finds a critical value of the cell side d below which some frequencies be-

come imaginary, i.e., the corresponding modes become unstable. For our system ($N=8$) the critical value is $d_2=0.969r_0$. We have compressed the system to a value slightly above d_2. In this case there are N^2 distinct frequencies $\omega^x_{hk}=\omega^y_{kh}$, ranging from 0.0658 to 8.4471. The relevant DOFs are thus the 64 group energies, where each group entails two modes:

$$E_{hk}=\frac{M}{2}[(\dot{q}^x_{hk})^2+(\omega^x_{hk}q^x_{hk})^2+(\dot{q}^y_{kh})^2+(\omega^y_{kh}q^y_{kh})^2] \ .$$

We have used a central-differences algorithm for the numerical integration of the equations of motion, improving the standard algorithm by one order in the velocities. A description of this modified algorithm is given in [8]. We have explored the energy range $e=0.2-0.002$, where e is the energy per particle $e=E/N^2$. For argon, this corresponds to temperatures in the range $24-0.24$ K, which includes the transition region determined in [3,4] for the 64-particle system. In this range we have studied the dynamics of the system at the energy values $e=0.2,0.05,0.02,0.007,0.002$. The total energy was initially distributed at random among all particles; as a consequence it was distributed at random among all normal modes.

We have computed the maximum Lyapunov exponent λ_1 vs energy e in both cases. In the first (uncompressed) case, the curve showing $\ln\lambda_1$ vs $\ln e$ is composed of two straight segments with different slopes. The SST, located at the point where the slope changes [1,2], is found around $e=0.02$. The curve for the compressed system does not show any change in slope. As the compressed system is more anharmonic than the uncompressed one, the SST is expected at a lower temperature; therefore, it must lie below the range of energies studied here.

The CAs have been computed for different initial conditions, either in tangent or in phase space, for all energies. They show, as expected, a very weak sensitivity to tangent space initial conditions: by lowering the energy e, the relative spread of their values increases from 10^{-6} at $e=0.2$ to 0.04 at $e=0.002$. In Fig. 1 the spectra of the CAs for the zero-pressure system at $e=0.002$, 0.02, 0.2 are reported. The normal modes groups are indexed in order of increasing frequency. The spectrum in the weak chaoticity region ($e=0.002$) exhibits a structure where group 1 has the lowest CA, while groups 3 and 6 have the highest ones. This latter result corresponds to the peculiar behavior of the same groups found before [4]: the energies of groups 3 and 6 are almost constant, because the energy exchanges of each of them with all other groups are extremely small. On the other hand, this confirms the meaning attributed to the CAs, from which we can infer that groups 3 and 6 exhibit the least chaotic behavior among all DOFs.

The spectrum at the SST ($e=0.02$) shows a monotonous increase of coherence with the frequency of the normal modes: at this energy groups 3 and 6 have lost their singular behavior. Raising the energy well above the SST ($e=0.2$), the various groups behave more similarly. But there is a feature common to the last two energies: the low frequency group is the most chaotic, the high frequency group is the most coherent. This seems to agree with an early intuition by Rayleigh and Jeans, who speculated that the exchange of

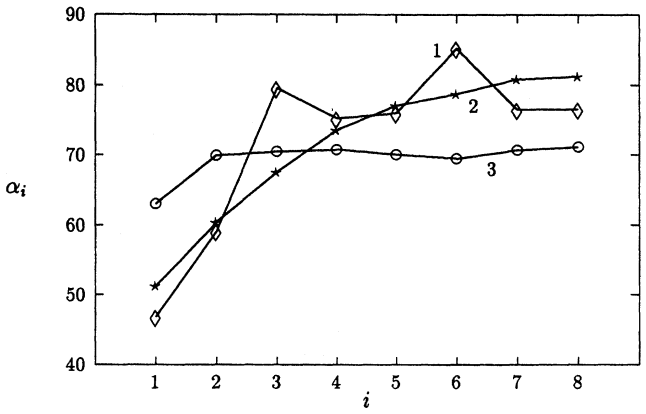

FIG. 1. Coherence angles for the uncompressed lattice at $e=0.002$ *(1)*, 0.02 *(2)*, 0.2 *(3)*. Each value is the average over three different initial conditions in the tangent space. The lines connecting the points are only an optical help. i is the index of the frequencies, which increase with i.

energy of a DOF would occur over times growing exponentially with its frequency; this guess has been later grounded through a theorem by Nekhoroshev [9,10].

In Fig. 2 the CAs vs e below and above the SST for the uncompressed lattice are reported: the spread of the $\alpha^{(l)}$ around the average value α diminishes when the energy is increased. Above the SST the CAs increase with the frequency of the corresponding group, while below the SST various crossovers take place. The smooth crossovers that seem to occur near the highest e are not significant, because at that energy the values of the CAs are affected by an uncertainty of about $\pm 1°$. So we could deduce that in the whole strong chaoticity region the DOFs are endowed with a degree of coherence which increases with their frequency—as long as their CAs are distinguishable.

This deduction turns out not to be valid in general. This is shown in Fig. 3, where the spectrum of the compressed lat-

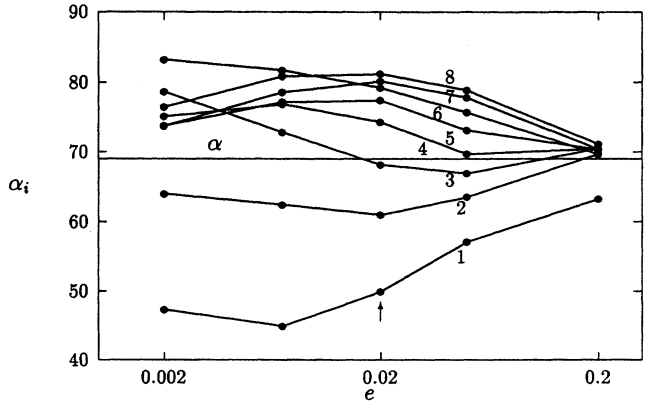

FIG. 2. Coherence angles for the uncompressed lattice vs e. The horizontal line corresponds to the average angle α. Labels on curves correspond to groups of different frequency. The arrow locates the SST.

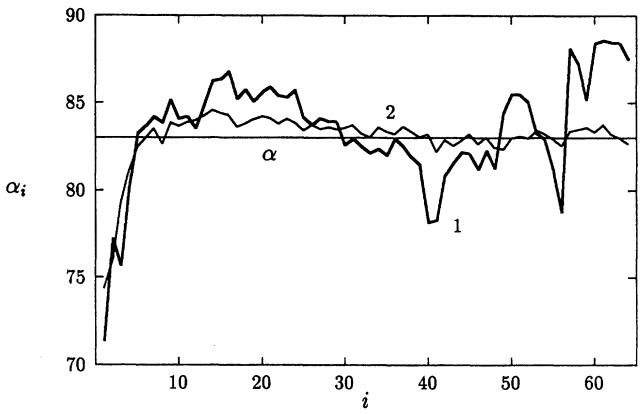

FIG. 3. Coherence spectrum for the compressed lattice at $e=0.002$ *(1)*, $e=0.05$ *(2)*. i is the index of the frequencies, which increase with i.

tice is reported, which gives a synoptic description of this system with many DOFs. The two curves correspond to the highest ($e=0.05$) and the lowest ($e=0.002$) energies studied. As said before, both energies should fall in the region of strong chaos, above the SST. In this case the average angle is $\alpha \simeq 83°$. At $e=0.002$, groups 1–8, which originate from group 1 at zero pressure, exhibit the lowest CAs, and the highest frequency groups are the most coherent, as expected [9,10]. But we found an unexpected high chaoticity of two medium or high frequency packets of groups centered around groups 40 and 56. At the higher energy the spectrum flattens, showing an almost homogeneous degree of chaoticity, again with the exception of the first eight groups. The coherence angles show here that even in this highly chaotic regime the different DOFs are characterized by different coherence levels. The high chaoticity of groups 40 and 56 may be related to the fact that their frequencies are resonant (within 0.4%) with the ratio 3/2.

We have also computed the CAs for a 3D zero-pressure system of $N^3=512$ particles, and found that their values were almost the same obtained for the 2D zero-pressure case [11]. To explain this, one can suppose that the degree of coherence of each group of normal modes—and hence the values of the CAs—should depend (for a given frequency) on the ratio between the number of coupling terms within each group of modes and the total number of coupling terms between the modes of one group and all others. The difference between the 2D and 3D zero-pressure cases of this ratio is only of the order of one per thousand [8]; of course this is only a quantitative hint, and this result deserves further investigation.

Let us make a final comment. In the last decade computer experiments have progressed towards the simulation of real systems with a large number of DOFs, while the main effort in the field of deterministic chaos has been devoted to low-dimensional and/or nonphysical systems. Up to now, therefore, there has been little cross-fertilization between these two fields. Nevertheless, when simulating a real system, one should also try to ascertain that the simulated system is endowed with the expected dynamical properties. In molecular dynamics computer experiments, for example, equilibrium time averages are assumed to be equivalent to ensemble averages. This is true if all DOFs behave chaotically, and in a similar way: this secures that the results are statistically meaningful, and do not depend on the initial state of the simulation. While the global indicators mentioned in the first paragraph do not give this information, the diagnostic tool presented here allows one to check easily how well this condition is met, also in systems with many DOFs.

We are indebted to G. Benettin, A. D'Aquino, G. Gallavotti, and R. Livi for enlightening discussions. One of us (M.D'A.) has been supported by a grant from the Forum of INFM.

[1] M. Pettini and M. Landolfi, Phys. Rev. A **41**, 768 (1990).
[2] M. Pettini and M. Cerruti-Sola, Phys. Rev. A **44**, 975 (1991).
[3] G. Benettin, G. Lo Vecchio, and A. Tenenbaum, Phys. Rev. A **22**, 1709 (1980).
[4] G. Benettin and A. Tenenbaum, Phys. Rev. A **28**, 3020 (1983).
[5] V. I. Osedelec, Trans. Moscow Math. Soc. **19**, 197 (1968).
[6] G. Benettin, L. Galgani and J. M. Strelcyn, Phys. Rev. A **14**, 2338 (1976).
[7] With an appropriate choice of the scalar product between phase space vectors, it is always possible to find the results we will obtain later, even when the subspaces are not orthogonal.
[8] M. D'Alessandro, A. D'Aquino, and A. Tenenbaum (unpublished).
[9] G. Benettin, L. Galgani, and A. Giorgilli, Phys. Lett. A **120**, 23 (1987).
[10] G. Benettin, L. Galgani, and A. Giorgilli, Nature (London) **311**, 444 (1984).
[11] In the 3D zero-pressure lattice the different frequencies are the same as in the 2D case, while the degeneration degree in each group is $3N/2=12$ times higher, so that each group entails 192 modes.